# Conformational Changes of Trialanine Induced by Direct Interactions between Alanine Residues and Alcohols in Binary Mixtures of Water with Glycerol and Ethanol

Siobhan Toal, Omid Amidi, and Reinhard Schweitzer-Stenner*

Departments of Chemistry, Drexel University, 3141 Chestnut Street, Philadelphia, Pennsylvania 19104, United States

S *Supporting Information*

ABSTRACT: Despite the increasing relevance of characterizing local conformational distributions in the unfolded state, an unambiguous description of the role that solvation and the addition of certain cosolvents play in altering this ensemble has yet to emerge. Alcohol cosolvents, and specifically glycerol, are known to act as protein stabilizers. The underlying mechanism of this effect is, however, still debated. Short alanine-based peptides provide a suitable model system for exploring the influence of cosolvents on backbone conformations, as ample experimental evidence now indicates that alanine does not exhibit a true statistical coil behavior but rather shows strong preference for sampling the polyproline II (PPII) region of the Ramachadran map when solvated in water. To explore the effect glycerol and ethanol cosolvents have on the conformational distribution of trialanine, we combined UV-CD and H NMR spectroscopies. The temperature dependence of the conformationally sensitive maximum dichroism ($\Delta\varepsilon$) and $^3J(H^\alpha H^N)$ coupling constants of two amide protons (N- and C-terminal) was subjected to a global thermodynamic analysis based on simple two-state PPII$\leftrightarrow\beta$ models. Interestingly, our results show that even small admixtures of alcohol (5% v/v) considerably change the spectral parameters, $\Delta\varepsilon_{PPII}$ and $\Delta\varepsilon_\beta$, as well as the enthalpic and entropic differences between the two states. For the central residue of trialanine in 5% glycerol, we obtained a gain in enthalpy favoring PPII of $\Delta\Delta H_n = -4.80$ kJ/mol and a compensating increase in entropy favoring the β-strand of $\Delta\Delta S_n = -13.53$ [J/mol K]. This causes increases in $-\Delta G$ and slight increases in PPII content. Further addition of alcohol, however, reverses the trend in that it causes a destabilization of the hydration shell and a shift toward β-strand conformations. The combined manifold of ΔH and ΔS values obtained for the investigated binary mixtures and the pure aqueous solvent exhibits an excellent linear correlation, which reflects enthalpy—entropy compensation and a common transition temperature. The latter can be considered an indication of a weak binding between cosolvent and peptide. A comparison of infrared and Raman spectra of trialanine in water and in water—alcohol mixtures indeed reveals a close proximity between aliphatic side chains of alanine residues and alcohol molecules even for 5% (v/v) alcohol—water mixtures. Hence, our results provide the first experimental evidence for direct interactions between, e.g., glycerol and peptides in aqueous solutions, in line with the result of recent calculations by Vagenende et al. (*Biochemistry* **2009**, *48*, 11084—11096) but at variance with preferential exclusion theories.
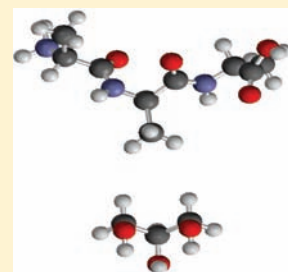
■ INTRODUCTION

The unfolded state of peptides and proteins has attracted considerable interest over the last 10—15 years for a variety of reasons. First, the discovery of the existence of so-called intrinsically disordered proteins and peptides (IDP) indicated that in contrast to a central dogma of modern biochemistry proteins do not necessarily have to adopt a well-defined secondary and tertiary structure to perform biological functions.[1—6] Second, some IDPs like α-synuclein and β-amyloid are involved in neurodegenerative diseases such as Parkinson's and Alzheimer's owing to their propensity for self-aggregation and fibril formation.[7—9] Third, experimental and theoretical evidence has been provided for the notion that the unfolded state is structurally less disordered than predicted by the statistical (or random) coil model,[9—23] which is built on the assumption that all amino acid residues besides proline can sample the entire sterically accessible region of the Ramachandran plot.[24—26] This notion seems to be particularly questionable for alanine, which is one of the most abundant amino acid residues in nature and exhibits the highest helical (right-handed) propensity of all amino acids.[27,28] Several lines of evidence resulting from circular dichroism, NMR, two-dimensional IR, as well as conventional IR and Raman experiments performed over the last ten years suggest that alanine has a strong preference for polyproline II (PPII) like conformations, which cover the right half of the upper left-hand quadrant of the Ramachandran plot (Figure 1).[20,21,29—34] The absolute number for the PPII propensity of alanine has been a matter of debate, ranging between 0.9 and ∼0.3,[23,33—38] with the latter number indicating that there is no special propensity for PPII at all. However, the most recent NMR and vibrational spectroscopy studies on polyalanines and the tripeptide GAG, in which the experimental data were analyzed in terms of realistic conformational distributions, unambiguously showed that the
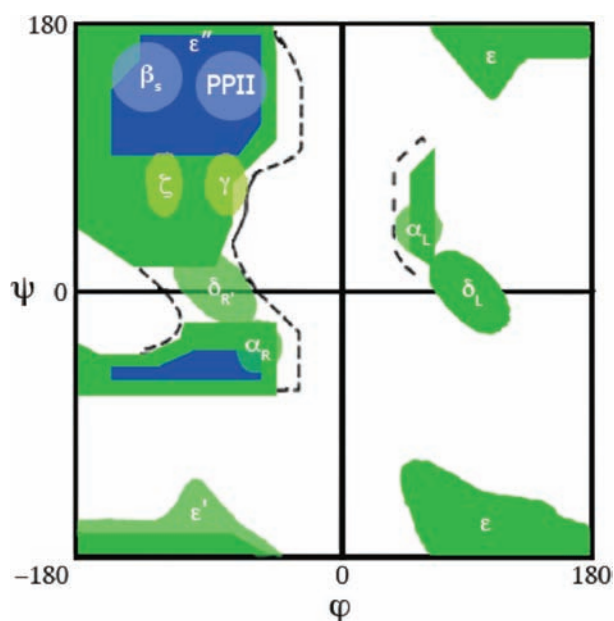
Figure 1. Ramachadran plot indicating the most accessible peptide/protein conformations. The Greek characters γ, δ, ε, and ξ label regions associated with various turn structures.

between 80 and 90% of alanine residues sample PPII-like conformations.[33,34,39,40] Hence, polyalanine peptides can exhibit local order (i.e., a polyproline II helix) even in the unfolded state of peptides and proteins. These experimental results are at variance with distributions obtained from Molecular Dynamics (MD) simulations of alanine-based peptides which generally underestimate the PPII propensity and overestimate the nucleation parameter of helix $\leftrightarrow$ coil transitions.[41−45] However, recent modifications of force fields and water models have moved the results of MD simulations closer to the above experimental values.[46−48]

The physical reason for the preferred sampling of the PPII trough by alanine has been debated in the literature. Results from a computational density functional theory (DFT) based study on the alanine dipeptide in explicit water (i.e., the peptide complexed with two and four water molecules), which appeared even before experimental evidence for the PPII preference of alanine was obtained, suggest that water stabilizes PPII by forming a bridge between adjacent carbonyl and amide groups by hydrogen bonding.[49] MD simulations of various polyalanines in explicit water with a modified Amber force field led Garcia to the conclusion that the PPII conformation is optimizing the packing of water molecules in the hydration shell of the peptide.[47] A somewhat similar rationale has been suggested by Kentsis et al. based on MD simulations of a series of GGXGG peptides.[50] They found that only alanine avoids a disruption of the backbone hydration shell, which explains why it seems to be the only residue with a high PPII propensity. A completely different explanation was given by Drozdov et al.[51] They performed MD and Monte Carlo simulations for the alanine dipeptide in explicit water and found that peptide—solvent interactions stabilize in fact compact conformations which do not include PPII. However, water enters the game by attenuating attractive electrostatic interactions between the peptide atoms. This leaves steric interactions as the decisive force for determining conformational preferences. PPII minimizes these interactions and thus becomes the most

prominent conformation. Drozdov et al. found no evidence for a role of H_2O bridges in stabilizing PPII. This notion was recently confirmed by Law and Dagett, who found that the occurrence of PPII conformations in proteins does not correlate with the existence of water bridges.[52]

All these different theories have in common that they emphasize the role of water and solvation for the stabilization of PPII. This notion seems to be in good agreement with experimental results. Eker et al., for instance, showed that the PPII content of the blocked AcAA—OH peptide is practically eliminated if water is replaced by DMSO as solvent.[53] Liu et al. used CD spectroscopy to investigate the solvent dependence of the conformational distributions of $AcGGAGGNH_2$.[54] They found that the PPII content of this peptide decreased in the order water > methanol > ethanol > 2-propanol, which reflects a linear correlation between PPII content and solvent polarity. The data did not reveal any correlation between the dielectric constant of the solvent and PPII, which is somewhat at odds with the model proposed by Drozdov et al.[51]

If water is indeed pivotal for the sampling of PPII conformations in unfolded peptides and proteins, the conformational distributions of the latter should be substantially altered by the addition of cosolvents. Theoretical and experimental studies aimed at describing the effect of certain cosolvents on protein/peptide conformations in aqueous solution have been performed thus far without providing an unambiguous picture. It is well established that protein stability can be enhanced with the admixture of kosmotropic cosolvents, such as polyols.[55−57] This induced stability can be described in terms of shifting conformational equilibria to more energetically favorable states. In addition, certain polyols such as glycerol have been shown to prevent protein aggregation, apparently by inhibiting partial unfolding or misfolding of aggregation-prone peptide segments.[56,57]

Typically, cosolvent-induced stabilization is discussed in terms of preferential hydration of the protein backbone by water or, similarly, preferential exclusion of cosolvent. Specifically, Gekko and Timasheff proposed that protein stabilization is a result of the preferential hydration of its backbone via exclusion of the glycerol cosolvent from the immediate domain of the protein.[55,56] More recently, Head-Gordon and co-workers analyzed data from neutron diffraction experiments on N-acetyl-leucine-methylamine (NALMA) in water and in a 1:5 glycerol—water mixture with an empirical potential structure refinement algorithm. Their results also suggest that glycerol preserves the peptide hydration shell.[58] In addition, this group performed MD simulations on the aforementioned system and observed that the population of water molecules in the solvation shell of the hydrophobic leucine residue increases in the presence of glycerol, while the peptide—H_2O hydrogen bonds are maintained.[59] These findings were found to be consistent with the results obtained from neutron diffraction data. However, a rather different picture emerged from a recent MD simulation of Vagenende et al. who investigated the proximity of glycerol molecules at the (hen egg white) lyzozyme-solvent interface in a glycerol—water mixture.[60] Their results suggest that two modes of protein—glycerol interactions are operative. One of them involves electrostatic interactions of a glycerol molecule with the protein surface, which induces an orientation of the solvent molecule so that further interactions between glycerols and protein groups are sterically inhibited. The second mode of interaction causes glycerol to preferentially interact with aliphatic groupings on the backbone, acting as an amphiphilic interface between the local hydrophobic surfaces on

the protein and the polar water solvent. This type of interaction has direct consequences for stabilizing aggregation-prone hydrophobic peptide segments in solution.

The above-cited work does not provide an unambiguous picture of how glycercol interacts with peptides and proteins. Clarifying this issue is of great importance for a variety of reasons. First, glycerol is used in numerous biophysical experiments on proteins (particularly those carried out at subzero temperatures) including protein-folding studies.[61,62] It is also routinely employed for protein crystallization[63] and in the food industry.[64] As indicated above, it stabilizes the folded state of proteins. However, if, in contrast to widespread thinking, glycerol does indeed interact directly with proteins and peptides, it is also necessary to determine how the cosolvent affects the Gibbs energy landscape of the unfolded state, which is much more exposed to the solvent than the folded state.

To shed some more light on how glycerol in particular and polyols in general affect the backbone structure of unfolded peptides, we investigated the influence of glycerol and ethanol on the conformational distribution of cationic trialanine in water. We choose trialanine as a simple model system for an unfolded peptide because its conformational propensities in pure aqueous solutions have recently been determined.[33,39] Ethanol was selected as an additional alcohol cosolvent for this study to make contact with a recent NMR/CD study on short unfolded peptides in binary mixtures of water and various alcohols.[54] Moreover, we deemed it useful to compare two cosolvents which differ in terms of their bulkiness and their number of aliphatic and polar groups. For our study, we combined ^{1}H NMR and far-UV-CD spectroscopy to determine how the conformational distribution of cationic trialanine in water is modified in mixtures of water with different amounts of ethanol and glycerol. All spectra were measured as a function of temperature. The resultant temperature dependence of the maximum dichroism measured at 215 nm and of the $^3J(H^N H^\alpha)$ coupling constants of two amide protons was subjected to a global analysis based on simple two-state models, from which the respective thermodynamic parameters (enthalpy and entropy) as well as the conformation specific spectroscopic parameters (i.e., average $\Delta\varepsilon$ and $^3J(H^N H^\alpha)$ of PPII and β-strand subensembles) were obtained. In addition, we recorded IR and polarized Raman spectra of trialanine for selected binary mixtures of the above cosolvents to identify possible interactions between the alcohol and peptide molecules. Our results clearly show that polar cosolvents affect the energy landscape of peptides. Moreover, they provide strong evidence for the notion that they interact directly with the aliphatic side chains. Our NMR data furthermore suggest that the thermodynamics of peptide−cosolvent interactions is different for the central and C-terminal residue of the peptide.

■ MATERIALS AND METHODS

Material. Alanyl-alanyl-alanine (AAA) was purchased from Bachem Bioscience, Inc. (>96% purity) and used without further purification. For UV-CD measurements, the peptide was dissolved in H_2O at a concentration of 5 mM. The same concentration was used for the binary mixtures of H_2O/ethanol (5%, 30%, 60% v/v) and H_2O/glycerol (5%, 30%, 60% v/v). The volume percentages of the binary mixtures correspond to the following mole fractions: 0.0134 and 0.016 for 5% glycerol and ethanol, 0.099 and 0.117 for 30% glycerol and ethanol, and 0.279 and 0.317 for 60% glycerol and ethanol, respectively. The sample was subsequently titrated with HCl to a pH value of 2.0. The choice of

the pH is critical to ensure on one side that nearly all peptides are in the cationic state, which requires a pH below 2.5, and on the other side to avoid a high Cl^- concentration (pH > 1.5), which would affect the absorbance below 200 nm. We have to confine ourselves to the cationic state to avoid the contributions from $n\rightarrow\pi^*$ and $\pi\rightarrow\pi^*$ charge transfer transitions from the carboxylate to the peptide group.[65] Using acidic conditions also facilitates the determination of $^3J(H^N H^\alpha)$ of the labile amide protons.

For IR and Raman experiments, the peptide was dissolved in mixtures of 5% ethanol and glycerol with D_2O at a concentration of 0.2 M. The solutions were titrated with DCl to a pD value of approximately 2.0. The pD values were determined by utilizing the method of Glasoe and Long[66] using an Accumet microsize standard glass electrode and pH meter (Fischer Scientific).

Peptide samples for H NMR experiments were diluted to a concentration of 50 mM in the appropriate binary mixture, using a 90% H_2O/ 10% D_2O (1% TMS) solution. The pH was again adjusted to approximately 2.0 with HCl.

UV-CD Spectroscopy. Temperature-dependent UV-CD spectra were obtained using a Jasco J-810 spectropolarimeter in the wavelength range of 190−300 nm. The sample was placed in a 100 μm ICl cell (International Crystal Laboratories) and into a nitrogen-purged system. Each sample was allowed to equilibrate to the desired temperature using a Peltier heating system (accuracy ± 1 °C). Spectra were recorded from 10 to 90 °C in increments of 10 °C with a 100 s delay time at each temperature and ten accumulations. The spectra were collected as ellipticity as a function of wavelength and converted to $\Delta\varepsilon$ [M^{-1} cm^{-1} res^{-1}]. For all UV-CD measurements, peptides were dissolved in H_2O or in the above-mentioned mixtures of H_2O and alcohols. The omission of the 10% D_2O, which we had to use for our NMR experiments, has a negligible effect ($\sim$2.9%) on the thermodynamic parameters derived from our experiments based on a comparison of UV-CD spectra of AAA in 100% H_2O and D_2O reported by Eker et al.[53]

Vibrational Spectroscopies. The experimental setup for FT-IR and Raman has been previously described in detail.[23,38] The FT-IR spectra were recorded with a Chiral IR Fourier Transform VCD spectrometer (BioTools). A cell (BioTools) with a path length of 100 μm was used for all experiments. The spectral resolution was 8 cm^{-1} for all measurements. Backgrounds of each acidic solvent (i.e., D_2O and all binary alcohol mixtures) were obtained separately and appropriately subtracted out of the final sample spectra.

All polarized Raman spectra were obtained with a 514 nm (800 mW) excitation from a Spectra Physics Argon−Krypton laser. The Raman-scattered light was collected in a backscattering geometry. The laser beam was directed into a RM 100 Renishaw confocal Raman microscope, and the scattered light was filtered with a 514 nm notch filter and polarized with a λ/2 plate. The light was dispersed by the spectrometer and then imaged onto a CCD (Wright Instruments). X-polarized spectra were recorded approximately 5 times, and y-polarized spectra were recorded approximately 10 times. All spectra were then averaged to sufficiently eliminate some of the noise. The same process was done for all AAA samples and solvent backgrounds. The resulting solvent spectra were then subtracted from the sample spectra using the previously described software MULTIFIT.[67]

^{1}H NMR Spectroscopy. Temperature-dependent ^{1}H NMR measurements were carried out on a 500 MHz Varian FT-NMR instrument equipped with a 5 mm HCN triple resonance probe. One-dimensional spectra were collected from 25 to 60 °C with 5 °C intervals. The sample temperature was controlled using Varian's VT controller. Varian's VNMR software (v. 6.1) was used to process all spectra, and the presaturation mode was used to suppress solvent signals. The sample was allowed to equilibrate for 100 s at each temperature, and 4−32 transients were collected for each, depending on the temperature
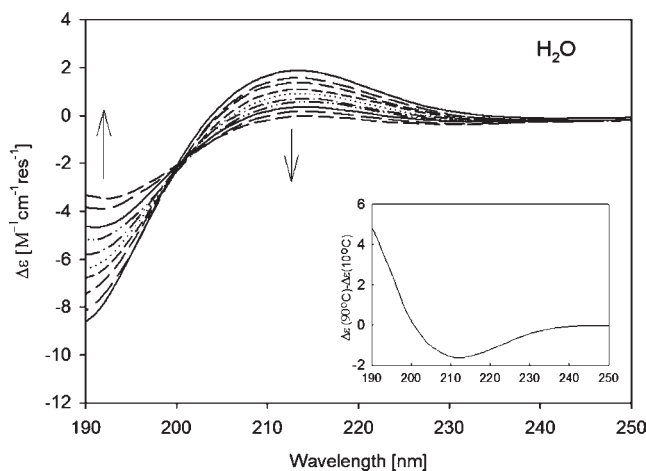
Figure 2. Temperature-dependent UV-CD spectra of cationic AAA in H_2O at pH 2.0. Arrows indicate increasing temperature from 0 to 90 °C. Inset: CD difference spectrum obtained by subtracting the spectrum measured at 10 °C from the spectrum recorded at 90 °C.

Figure 3. Maximum dichroism ($\Delta\varepsilon_{215 \text{ nm}}$) obtained from the UV-CD spectrum of cationic AAA in H_2O plotted as a function of temperature from 273 to 363 K.

(the highest temperatures generally required 32 scans). Phase correction of initial spectra was performed using Mestrec software, and all $^3J(H^N,H^\alpha)$ were determined via deconvolution and fitting of the amide proton signals using MULTIFIT software with Lorentzian band profiles. To obtain accurate values for $^3J(H^N,H^\alpha)$ coupling constants at all temperatures and solvation conditions, the following procedure was carried out. The temperature dependence of the peak position (Hz) of individual bands of the obtained amide proton doublets was subjected to a linear regression analysis. The $^3J(H^N,H^\alpha)$ splitting of a spectral signal measured at a certain temperature was then determined by subtracting the respective chemical shift values of the linear fits. An explanatory example for this procedure can be found in the Supporting Information (Figures S1 and S2).

■ RESULT AND DISCUSSION

This section is organized as follows. First, we reanalyze the temperature dependence of the UV-CD spectrum and the $^3J(H^N,H^\alpha)$ constants of trialanine in water by means of a global fitting procedure based on a two-state model. This procedure is facilitated by the results obtained from a recent analysis of the conformational manifold which this peptide exhibits at room temperature and yields the enthalpic and entropic difference between the considered states.[33,39] In a second step, we use the results of this analysis as a starting point to determine the conformational ensemble sampled by trialanine in binary mixtures of water with glycerol and ethanol at different temperatures and to characterize the obtained ensembles in thermodynamic terms.

AAA in Water. In a first step, we remeasured the far UV-CD spectra of cationic trialanine in water as a function of temperature between 10 and 90 °C, which are shown in Figure 2. The inset depicts the difference spectrum calculated by subtracting the spectrum recorded at 10 °C from that measured at 90 °C. At low temperatures, the pronounced positive maximum of the CD spectrum at approximately 215 nm is diagnostic of a dominant sampling of PPII-like conformations, in agreement with what has been now well-established in the literature.[68,69] The difference spectrum indicates a change of the conformational distribution from PPII-like to more extended β-strand-like conformations, again in agreement with earlier results.[70] The maximum dichroism ($\Delta\varepsilon$) at approximately 215 nm decreases with increasing
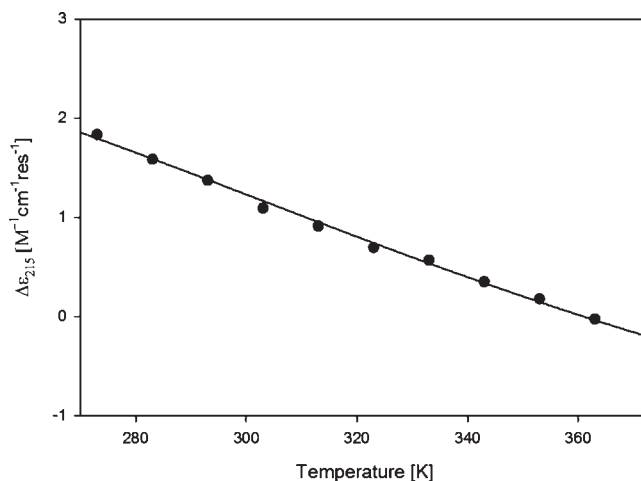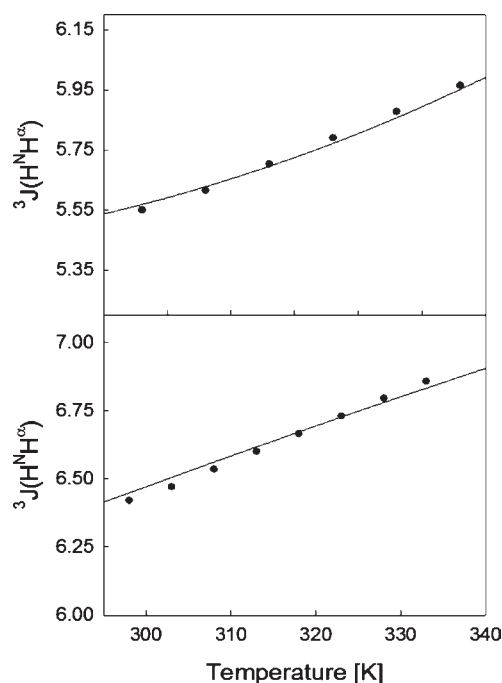

Figure 4. Temperature dependence of the $^3J(H^NH^\alpha)$ coupling constants of cationic AAA in H_2O obtained from the NMR signals of the N-terminal (upper panel) and C-terminal (lower panel) amide protons. The solid lines represent fits of a two-state model discussed in the text.

temperature as shown in Figure 3, also reflecting this shift from PPII to β states.

Although UV-CD is a powerful tool for obtaining qualitative information on the conformational ensemble of the population as a whole, residue-specific information is lacking. To obtain residue-level details about the peptide conformations, we performed ^1H NMR spectroscopy for cationic trialanine in water and determined the C-terminal and N-terminal $^3J(H^N,H^\alpha)$ coupling constants as a function of temperature (Figure 4). Here, we utilized the nomenclature of Oh et al., who termed the coupling constant reflecting the φ-angle of the central alanine
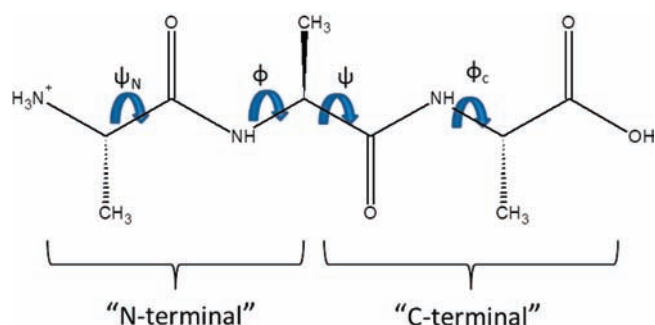
Figure 5. Cationic trialanine with N-terminal and C-terminal outlined for reference. For H NMR analysis, it is necessary to consider two amide protons resulting in two $^3J(\mathrm{H^N,H^\alpha})$ values associated with two different ϕ values (ϕ_N and ϕ_C). ϕ_N is associated with the central alanine residue or "N-terminal". Ψ_n is associated with the "C-terminal" alanine residue.

residue of the peptide as "N-terminal".[71] This reflects the fact that the N-terminal alanine is not associated with an amide proton (Figure 5). The $^3J(\mathrm{H^N,H^\alpha})$ coupling is sensitive to changes in the dihedral angle ϕ of the respective residue as described by the Karplus equation.[72] The experimentally determined value for the N-terminal coupling constant increases in the temperature range studied from 5.53 to 6.14 Hz in good agreement with experimental studies by Graf et al.[39] These values are also indicative of a change in the conformational equilibrium between PPII= to more β-like distributions. The experimental coupling for the C-terminal ranges from 6.4 to 6.86 Hz, which is also in agreement with literature values.[39]

Two-State Models. These temperature-dependent dichroism and $^3J(\mathrm{H^N,H^\alpha})$ values indicate a change in the conformational distribution sampled by trialanine. It has recently been shown that this ensemble can be described as a superposition of two-dimensional Gaussian distributions located at the PPII, β-strand, right-handed helical, and γ-turn troughs of the Ramachandran plot.[33] Here, we neglect the small fractions of helical and turn structures, thus confining ourselves to PPII and β-strand like conformations. The experimentally measured values of $\Delta\varepsilon$ and $^3J(\mathrm{H^N,H^\alpha})$ can then be represented by mole fraction weighted (χ_{PPII} and χ_β) contributions from each conformation as follows

$$\Delta\varepsilon(T) = \chi_{\mathrm{PPII}}\Delta\varepsilon_{\mathrm{PPII}} + \chi_\beta\Delta\varepsilon_\beta \tag{1}$$

$$\Delta J(T) = \chi'_{\mathrm{PPII}}J_{\mathrm{PPII}} + \chi'_\beta J_\beta \tag{2}$$

where $\Delta\varepsilon_{\mathrm{PPII}}$, J_{PPII}, $\Delta\varepsilon_\beta$, and J_β denote the respective average dichroism and coupling constants of PPII and β-strand conformations, respectively. The mole fractions in eq 2 are labeled as χ' because they are different from those used to describe $\Delta\varepsilon$ in eq 1 for reasons described below.

Elementary statistical mechanics allows one to express the mole fractions in eqs 1 and 2 in terms of Boltzmann factors. For $\Delta\varepsilon$ values measured as a function of temperature at a distinct wavelength, this yields

$$\Delta\varepsilon = \frac{(\Delta\varepsilon_{\mathrm{PPII}} + \Delta\varepsilon_\beta e^{\Delta G/RT})}{1 + e^{\Delta G/RT}} \tag{3}$$
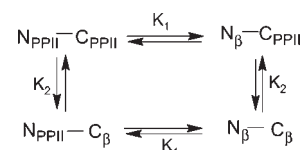
where $\Delta G = G_{\mathrm{PPII}} - G_\beta$ represents the Gibbs free energy difference between these two peptide conformations; R is the gas constant; and T is the absolute temperature. The model

described by eq 3 is an oversimplification in many regards. Because the CD spectra do not provide site-specific information, their analysis was based on the assumption that the behavior of the entire peptide is describable by a two-state model, for which all residues exhibit either PPII or β-strand. Even though it is well established that the PPII$\leftrightarrow\beta$ transition is noncooperative,[31] this assumption seems to be justified by the very fact that the spectra in Figure 2 display an isodichroic point at approximately 200 nm. This is most likely due to the fact that both residues provide nearly identical contributions to the observed dichroic value if they adopt similar conformations, in line with results from a recent theoretical study of Woody.[69] The applicability of a two-state model for explaining the CD spectra of trialanine has also recently been demonstrated by Oh et al.[71] Hence, with respect to the CD data, the term "two-state model" is referring to two different states of the entire peptide. This implies that peptides with mixed residue conformations (e.g., PPII for the central and β-strand for the C-terminal residue) are treated like a 50:50 mixture of pure PPII and β-strand peptides.

While the temperature-dependent CD spectra have to be analyzed in terms of two net peptide conformations, the site-specific information provided by the NMR data permits the use of a more realistic model which involves four conformations of trialanine based on a *two-state model for individual residues*.[71] A tripeptide contains two peptide bonds and hence two corresponding pairs of (ψ,φ) values that describe the local secondary structure of the central and C-terminal alanine residue. The above-mentioned two-state model can now be formulated for each individual residue, which is thus considered able to adopt two conformations, β or PPII. Hence, the temperature dependence of the corresponding $^3J(\mathrm{H^N,H^\alpha})$ can be written as

$$J_i(T) = \frac{J_{\mathrm{PPII},i} + J_{\beta,i}e^{\Delta G_i/RT}}{(1 + e^{\Delta G_i/RT})} \tag{4}$$

where $i = \mathrm{N,C}$ indicates the amide proton for which $^3J(\mathrm{H^N,H^\alpha})$ is calculated. To relate the site-specific Gibbs free energies in eq 4 with the apparent ΔG in eq 3, we have to consider the following thermodynamic scheme:

$$\begin{array}{ccc}
\mathrm{N_{PPII}{-}C_{PPII}} & \underset{}{\overset{K_1}{\rightleftarrows}} & \mathrm{N_\beta{-}C_{PPII}} \\
K_2 \big\updownarrow & & \big\updownarrow K_2 \\
\mathrm{N_{PPII}{-}C_\beta} & \underset{K_1}{\rightleftarrows} & \mathrm{N_\beta{-}C_\beta}
\end{array}$$

where K_1 and K_2 denote the equilibrium constants of the PPII$\leftrightarrow\beta$ transitions of the central residue (probed by the N-terminal coupling constant) and C-terminal residue, respectively. For this model, a straightforward calculation using mass action law relates the two site-specific equilibrium constants K_1 and K_2 to the effective equilibrium constant associated with ΔG in eq 3[71]

$$K = \frac{2K_1K_2 + K_1 + K_2}{2 + K_1 + K_2} \tag{5}$$

A global analysis of $\Delta\varepsilon(T)$ and $^3J(\mathrm{H^N,H^\alpha})(T)$ was based on the statistical distribution obtained for the central residue of trialanine at room temperature.[33] This way, the average $^3J(\mathrm{H^N,H^\alpha})$ coupling value pertaining to each subdistribution (i.e., J_{PPII}, J_β) could be determined utilizing the newest version of the empirical

Table 1. (a) Spectroscopic Parameters Obtained from Global Fitting of the Temperature Dependence of $^3J(H^N,H^\alpha)$ Coupling Constants and $\Delta\varepsilon_{215\ nm}$ of Cationic AAA in H_2O and (b) Thermodynamic Parameters Obtained from Global Fitting of the Temperature Dependence of $^3J(H^N,H^\alpha)$ Coupling Constants Obtained for N- and C-Terminal Amide Protons and of the Corresponding Temperature Dependence of $\Delta\varepsilon_{215\ nm}$ of Cationic AAA in H_2O

(a)							
$^3J_n(H^\alpha H^N)$ [Hz][a]	$J_n(PPII)$ [Hz]	$J_n(\beta)$ [Hz]	$^3J_c(H^\alpha H^N)$ [Hz][a]	$J_c(PPII)$ [Hz]	$J_c(\beta)$ [Hz]	$\Delta\varepsilon_{PPII}$ [$M^{-1}\ cm^{-1}\ res^{-1}$]	$\Delta\varepsilon_\beta$ [$M^{-1}\ cm^{-1}\ res^{-1}$]
5.53	5.29	9.27	6.40	5.28	9.27	2.45	−3.68

(b)							
$\chi_n(PP2)$	ΔG_n [kJ/mol]	$\chi_c(PP2)$	ΔG_c [kJ/mol]	ΔH_n [kJ/mol]	ΔH_c [kJ/mol]	ΔS_n [J/mol K]	ΔS_c [J/mol K]
0.94	−6.71	0.72	−2.32	−30.43	−10.15	−79.60	−26.29

[a] Experimental $^3J(H^N,H^\alpha)$ at 298 K.

Karplus relationship.[39] Using these values as a reference in eq 2 along with the experimental room-temperature values for $^3J(H^N,H^\alpha)$ of each residue, the respective mole fractions χ_{PPII} could be obtained (Table 1). Thus, we derived χ_{PPII} values of 0.94 and 0.72 for the central residue (N-terminal) and the C-terminal residue, respectively. The different PPII content obtained for the two residues could be expected since the peptide and carboxylate groups provide different nearest-neighbor environments and thus also a different structure of the hydration shell. Our results are in line with what has been previously reported by Oh et al.[71] Next, the above mole fractions were used to calculate the Gibbs free energy differences $\Delta G_{N,C}$ between the two residues' conformations at room temperature T_r. The respective values were then used to relate the enthalpic and entropic difference between the two conformations, which finally lead to the following equation used for our analysis

$$J_i = \frac{J_{PPII,i} + J_{\beta,i}e^{\beta_i/RT}}{(1 + e^{\beta_i/RT})} \qquad (6)$$

with

$$\beta_i = \Delta H_i - T \cdot \left(\frac{\Delta H_i - \Delta G_r}{T_r}\right) \qquad (7)$$

where ΔG_r is the Gibbs free energy difference at room temperature T_r. Using eqs 6 and 7, the temperature-dependent $^3J(H^N,H^\alpha)$ coupling constants for the center residue could be fit using solely ΔH as a free parameter (eq 2). A fine-tuning of the fits required subtle changes of $J_{PPII,i}$. The results of the fits were used to determine the respective equilibrium constants (K_1 and K_2) for each residue, which were then employed in eq 5 to calculate the effective equilibrium constant (K) and thus the effective thermodynamic parameter ΔG. From the temperature dependence of ΔG, the corresponding values for ΔH and ΔS for the central residue of cationic trialanine in water were obtained (i.e., $\Delta H_n = -30.43$ kJ/mol and $\Delta S_n = -79.6$ J/mol K). The parameter values thus obtained are listed in Table 1. The final fit to the $\Delta\varepsilon(T)$ data which was then carried out with eq 3 and $\Delta\varepsilon_{PPII}$ and $\Delta\varepsilon_\beta$ as free parameters is displayed as a solid line in Figure 3. The respective values for $\Delta\varepsilon_{PPII}$ and $\Delta\varepsilon_\beta$ are listed in Table 1.

The value for ΔH and the respective entropy value are larger than what Eker et al. earlier reported based on a somewhat different analysis, which was not restricted by site-specific experimental information about individual residues.[73] Since the

entropic contribution to the Gibbs energy favors the β-strand conformation, they obtained a much lower PPII fraction of ca. 0.5. Oh et al., by decomposing the CD spectra of cationic trialanine into basis spectra by singular value decomposition and a simultaneous analysis of $^3J(H^N,H^\alpha)$, obtained a ΔH of ca. 12.5 kJ/mol and a ΔS of 25 J/K mol The corresponding propensity for PPII at room temperature would be 0.97, which is higher than the experimental value determined from the analyses of various J-coupling constants and amide I profiles.[33] Graf et al. measured several J coupling constants reflecting the conformational distribution of the central amino acid residue of AAA as a function of temperature. Their analysis yielded a ΔH of ca. 25.1 kJ/mol and a ΔS of 62 J/K mol.[39] Both values are lower than what we obtained from our data. The respective PPII propensity of alanine at room temperature would be 0.9, which is slightly lower than our value. It should be noted in this context that at high propensity values (i.e., > 0.8) modest uncertainties for the determination of mole fractions transfer into comparatively large errors for the underlying thermodynamic parameters.

The comparison of the thermodynamic parameters obtained from different reported experiments still reveals some discrepancies, though all clearly suggest that PPII is enthalpically favored, while the entropy stabilizes β-strand-like conformations. The PPII fractions of the central residue at room temperature reported by Graf et al.[39] and Schweitzer-Stenner[33] are slightly lower than the value used for the above analysis. Since we found that fits based on lower PPII propensity at room temperature than 0.94 are of lesser quality than the one shown in Figures 3 and 4, we stick to this value for calibrating the analysis of our CD spectra.

AAA in Binary Mixtures. Figure 6 exhibits the UV-CD spectra of two ethanol/water and three glycerol/water mixtures as a function of temperature (we also measured the CD spectra for a 60% water−ethanol spectrum; however, we could not obtain good NMR spectra for this mixture, so we omitted the respective CD data in Figure 6). In the region below 200 nm, some of these spectra are somewhat noisier than those of AAA in pure water, which might be due to impurity scattering or high solvent absorptivity. However, this was not too much of a concern because we used again the maximum $\Delta\varepsilon$ at approximately 215 nm for our thermodynamic analysis. The corresponding $\Delta\varepsilon(T)$ plots, as well as the temperature-dependent $^3J(H^N,H^\alpha)$ coupling for each binary mixture, are all shown in Figure 7 and Figure 8, respectively. The solid lines all result from fitting the data using the aforementioned fitting routine. The temperature-dependent decrease in the maximum dichrism $\Delta\varepsilon_{215}$ indicates decreased
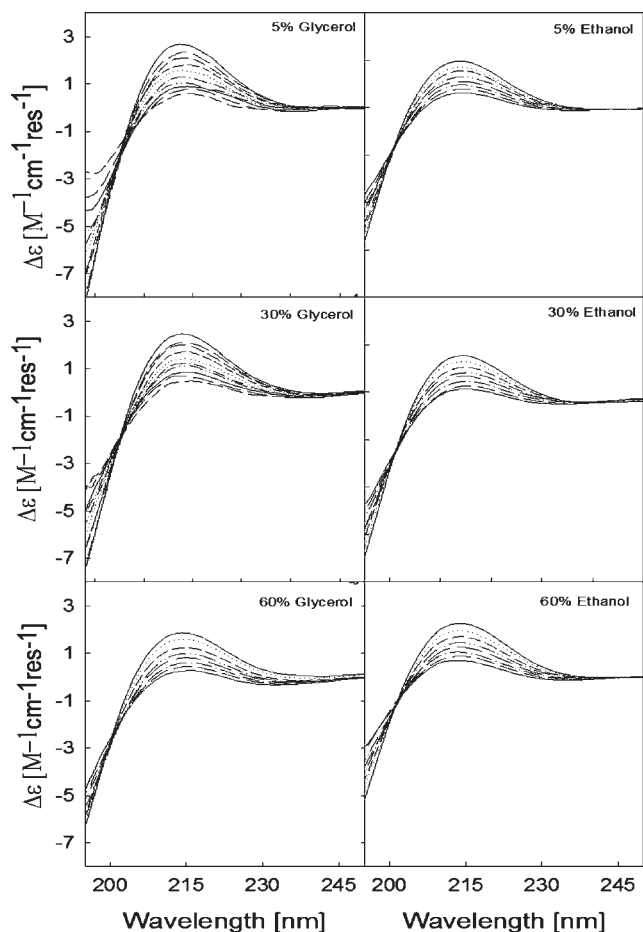
Figure 6. Temperature dependence of UV-CD spectra of cationic AAA in glycerol/H$_2$O and ethanol/H$_2$O binary mixtures. Upper panel: 5% binary mixtures. Middle panel: 30% binary mixtures. Lower panel: 60% binary mixtures.
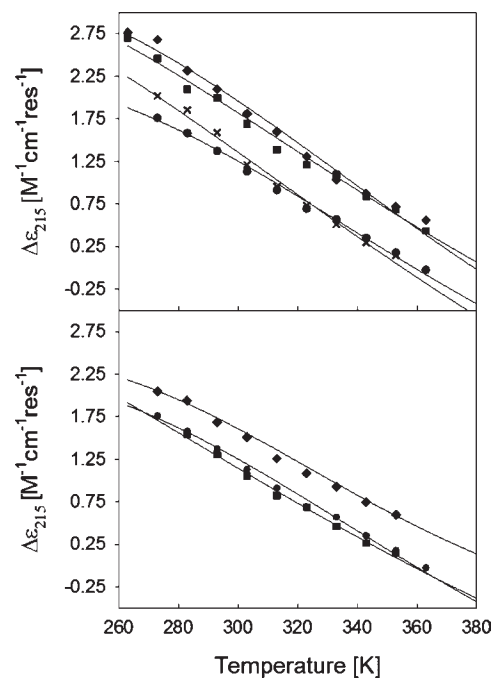

Figure 7. Maximum UV-CD ($\Delta\varepsilon_{215}$) signal plotted as a function of temperature from 273 to 363 K for AAA in binary mixtures. The solid lines result from fitting procedures described in the text. Glycerol binary mixtures (upper panel): D$_2$O (circles), 5% glycerol (diamonds), 30% glycerol (squares), and 60% glycerol (crosses). Ethanol binary mixtures (lower panel): D$_2$O (circles), 5% ethanol (diamonds), 30% ethanol (squares).

PPII content as a function of increasing temperature, in line with what was found above for pure water. The $^3J(H^N,H^\alpha)$ coupling constants for all solvent mixtures increase as a function of temperature, also signifiying an increased sampling of β-like conformations in the ensemble. Interestingly, at room temperature the experimentally determined $^3J(H^N,H^\alpha)$ values for AAA in ethanol/water and glycerol/water at the same volume percent are nearly identical, i.e., $^3J(H^N,H^\alpha)$ = 5.45 Hz for 5% admixtures alcohol and $^3J(H^N,H^\alpha)$ = 5.77 Hz for 30% admixtures alcohol. However, the temperature coefficients for the $^3J(H^N,H^\alpha)$ values of each mixture are different for the two alcohols, thus indicating a different Gibbs energy landscape and more pronounced differences between corresponding conformational mixtures at higher temperatures. The increase of $^3J(H^N,H^\alpha)$ with temperature is generally more pronounced for water/ethanol as compared to water/glycerol mixtures, indicating that the conformational distribution of AAA shifts toward higher β content for ethanol more efficiently then for AAA in glycerol mixtures.

The resulting thermodynamic and conformation specific spectroscopic parameters determined from the fitting routine are all listed in Table 2. We interpreted the obtained changes of $\Delta\varepsilon_{PPII}$ and $\Delta\varepsilon_\beta$ as indicative of changes of the distribution of PPII and β-strand-like conformations, which could involve changes of the coordinates of the distribution center as well as

alterations of the distribution widths. However, a successful fitting of our data did not require changes of J_β and only rather small changes of J_{PPII}, which seems to be at variance with the changes observed for $\Delta\varepsilon_\beta$ and $\Delta\varepsilon_{PPII}$. One possible explanation of these conflicting observations is that the obtained changes of $\Delta\varepsilon$ solely reflect variations along the ψ-coordinate, which would not affect $^3J(H^N,H^\alpha)$. Additionally, we could invoke changes of the halfwidth of the Gaussian distribution along ϕ and ψ. Changing the halfwidth with respect to ϕ would not drastically change $^3J(H^N,H^\alpha)$ because the relationship between $^3J(H^N,H^\alpha)$ and ϕ is nearly linear for ϕ-values between $-60°$ and $-100°$. The $\Delta\varepsilon$ values in Table 2 suggest that even small amounts (i.e., 5%) of the two cosolvents cause significant changes of $\Delta\varepsilon_{PPII}$ and $\Delta\varepsilon_\beta$. Glycerol is more effective in changing $\Delta\varepsilon_{PPII}$ than ethanol, whereas the latter has a rather strong effect on $\Delta\varepsilon_\beta$.

The admixture of alcohol to water has also had a substantial impact on the thermodynamic parameters of the system but surprisingly much less influence on the PPII propensities of the two alanine residues. The χ_{PPII} values slightly increase upon the addition of 5% alcohol and decrease to a somewhat larger extent if the alcohol content is 30% or greater. The discordance between the rather drastic changes of both ΔH and ΔS and the modest change of χ_{PPII} which we obtained even for a 5% admixture of alcohol reflects a rather interesting compensation between $\Delta\Delta H$ and $\Delta\Delta S$ (these differences are calculated by subtracting the value obtained for the pure water solvent from the respective value of the binary mixture). This can be illustrated by comparing the respective values for 5% admixture glycerol (Table 2). For the central residue, we obtained $\Delta\Delta H_n = -4.8$ kJ/mol and $\Delta\Delta S_n = -13.5$ J/mol K. Hence, the gain in enthalpy (favoring PPII) is
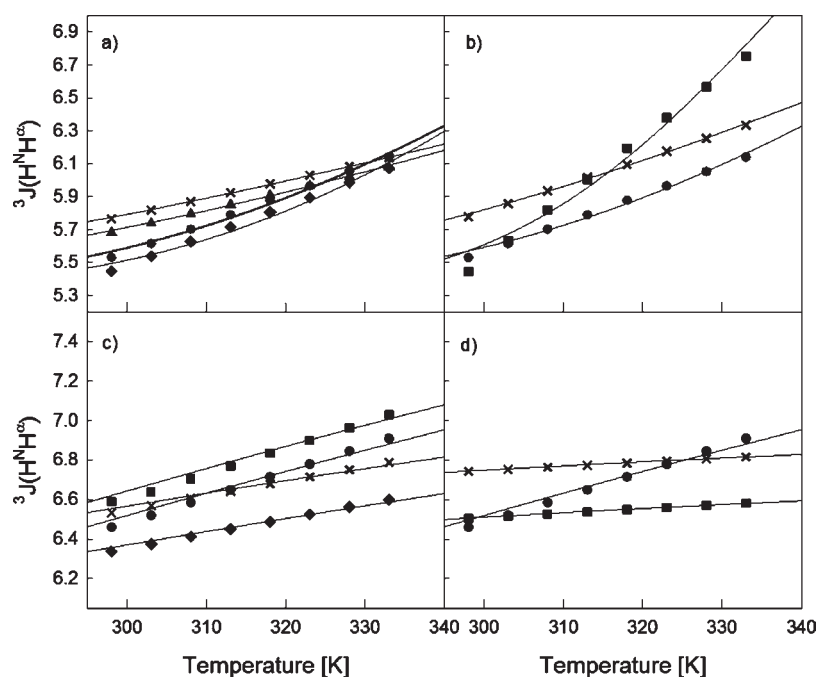
Figure 8. $^3J(H^\alpha H^N)$ [Hz] of N-terminal (upper panels) and C-Terminal (lower panels) plotted as a function of temperature from 298 to 333 K for AAA in binary mixtures. The data for glycerol/H_2O mixtures are shown in the left panel, and the data of the corresponding ethanol/H_2O mixtures are displayed in the right panels. Parts (a) and (c) show the data for H_2O (circles), 5:95 glycerol:H_2O (diamonds), 30:70 glycerol:H_2O (crosses), 60:40 glycerol:H_2O (triangles). Parts (b) and (d) show the data for H_2O (circles), 5:95 ethanol:H_2O (squares), and 30:70 ethanol:H_2O (crosses).

Table 2. (a) Spectroscopic Parameters Obtained from Global Fitting of the Temperature Dependence of $^3J(H^N, H^\alpha)$ Coupling Constants Obtained for N- and C-Terminal Amide Protons and of $\Delta\varepsilon_{215nm}$ of Cationic AAA in Binary Mixtures and (b) Thermodynamic Parameters Obtained from Global Fitting of the Temperature Dependence of $^3J(H^N, H^\alpha)$ Coupling Constants Obtained for N- and C-Terminal Amide Protons and of the Corresponding Temperature Dependence of $\Delta\varepsilon_{215nm}$ of Cationic AAA in Binary Mixtures

(a)				
solvent[b]	$^3J(H^N, H^\alpha)$ [Hz][a]	J_n(PPII) [Hz]	$\Delta\varepsilon_{PPII}$ [M^{-1} cm^{-1} res^{-1}]	$\Delta\varepsilon_\beta$ [M^{-1} cm^{-1} res^{-1}]
5:95 glycerol/H_2O	5.45	5.27	3.60	−5.10
30:70 glycerol/H_2O	5.77	5.32	3.76	−4.93
60:40 glycerol/H_2O	5.69	5.32	3.74	−7.78
5:95 ethanol/H_2O	5.45	5.23	2.58	−1.93
30:70 ethanol/H_2O	5.78	5.33	3.53	−6.09

(b)							
solvent[b]	χ_n (PPII)	$\Delta\Delta G_n$ [kJ/mol]	χ_c (PPII)	$\Delta\Delta G_c$ [kJ/mol]	$\Delta\Delta H_n$ [kJ/mol]	$\Delta\Delta H_c$ [kJ/mol]	$\Delta\Delta S_n$ [J/mol K]	$\Delta\Delta S_c$ [J/mol K]
5:95 glycerol/H_2O	0.96	−0.76	0.75	−0.37	−4.80	3.48	−13.53	12.92
30:70 glycerol/H_2O	0.89	1.69	0.69	0.36	14.80	−3.18	57.52	−0.19
60:40 glycerol/H_2O	0.91	1.13	0.70	0.23	11.61	4.28	35.16	13.56
5:95 ethanol/H_2O	0.95	−0.30	0.71	0.15	−18.74	7.98	−61.87	26.28
30:70 ethanol/H_2O	0.89	1.71	0.65	0.83	9.25	8.33	25.31	25.19

^{a} Experimental $^3J(H^N, H^\alpha)$ at 298 K. ^{b} All solvent compositions are (v/v) percents.

nearly compensated for by the increase of the entropic difference, which takes away nearly 4 kJ/mol at room temperature.

The changes of thermodynamic parameters and PPII content are not monotonous with respect to increasing cosolvent fractions. As indicated above, even the addition of 5% alcohol causes the negative free energy difference ($−\Delta G$) to *increase* for both

central and C-terminal residues (Table 2). However, this effect becomes reversed for 30:70 alcohol−water mixtures for which $\Delta\Delta G$ becomes positive. Interestingly, in a separate analysis we found that the temperature coefficients of the chemical shifts for both amide protons also show this nonmonotonous behavior with respect to increasing cosolvent concentration (Figures S2−S7,
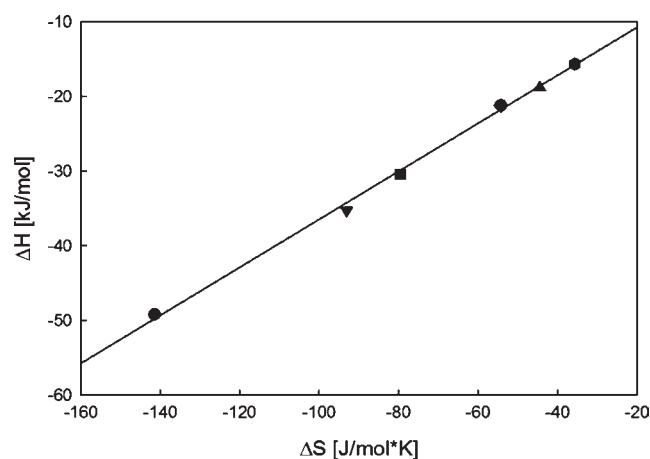
12735

dx.doi.org/10.1021/ja204123g |*J. Am. Chem. Soc.* 2011, 133, 12728–12739

Figure 9. Correlation of ΔH and ΔS values obtained from a thermodynamic analysis of $^3J(H^\alpha H^N)$ coupling constants reflecting the ϕ-values of the central residue of AAA in water, glycerol/water, and ethanol/water binary mixtures. Individual points are assignable as follows: pure H_2O (square), 5% glycerol (upside down triangle), 30% glycerol (hexagon), 60% glycerol (triangle), 5% ethanol (circle), and 30% ethanol (ellipse). The solid line results from a linear regression to the data, which is described in the text.
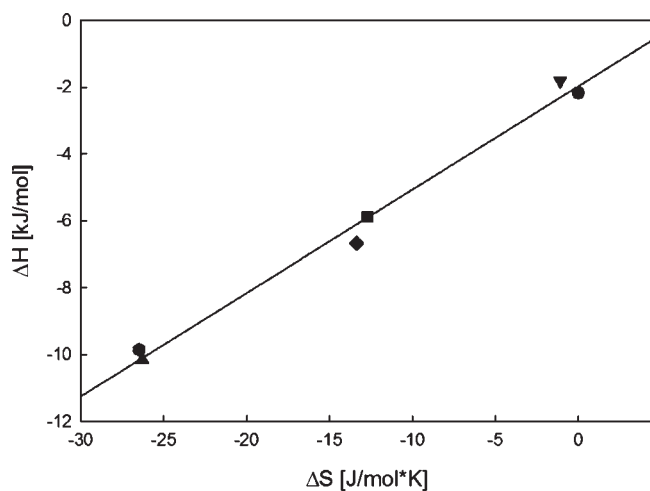
Figure 10. Correlation of ΔH and ΔS values obtained from a thermodynamic analysis of $^3J(H^\alpha H^N)$ coupling constants reflecting the ϕ-values of the C-terminal residue of AAA in water, glycerol/water, and ethanol/water binary mixtures. Individual points are assignable as follows: pure H_2O (square), 5% glycerol (upside down triangle), 30% glycerol (hexagon), 60% glycerol (triangle), 5% ethanol (circle), and 30% ethanol (ellipse). The solid line results from a linear regression to the data, which is described in the text.

Supporting Information). The values for $\Delta\Delta H$ and $\Delta\Delta S$ inferred from the temperature dependence of $^3J(H^N,H^\alpha)$ seem again to indicate an enthalpy—entropy compensation. To clarify whether the latter is characteristic for our peptide—solvent system, we plotted ΔH as a function of ΔS for both the N-terminal and the C-terminal residue. For each residue, we included the ΔH and ΔS values of all peptide—solvent mixtures investigated. The plots in Figures 9 and 10 suggest a linear relationship. Therefore, we fitted the equation

$$\Delta H = \Delta H_0 - T_{R'}\Delta S \qquad (9)$$

Table 3. Results Obtained from the Linear Fit of Enthalpy—Entropy Data[a]

residue	ΔH_o [kJ/mol]	T_R [K]	R^2
N-terminal	−4.28	321.5	0.997
C-terminal	−1.96	309.2	0.989

[a] Transition temperature, zero-point enthalpy, and correlation coefficient for the N- and C-terminal.

to the experimental data. Here, $T_{R'}$ is a reference temperature which is close but not identical to the above introduced transition temperature at which total compensation of enthalpic and entropic contributions is obtained (i.e., $\Delta G = 0$), whereas ΔH_0 can be understood as a zero-point enthalpy difference. We obtained excellent correlation coefficients for both plots and somewhat different T_R and ΔH_0 for the two residues (all listed in Table 3). This reflects the different (peptide) environment of the two residues (peptide—peptide for the central and peptide—carboxylic acid for the C-terminal residue). Further implications of the thus established enthalpy—entropy compensation, which can be described as a general property indicative of weak intermolecular interactions, will be discussed below.

Looking at the influence of cosolvent addition on the N- and C-terminal residue individually reveals that changing the alcohol content of the mixture affects the enthalpic and entropic contributions to the residues' Gibbs free energy rather differently. By adding 5% glycerol, for instance, the $-\Delta G$ value of both residues increase. However, the enthalpy difference between central residue conformers increases, whereas it decreases for the C-terminal conformers. As indicated above, the entropy change reduces the respective changes of the Gibbs energy. This observation corroborates the notion that the residue—solvent interactions of the two residues are qualitatively different. However, the enthalpy—entropy compensation ensures that the Gibbs energies and thus also the mole fractions of PPII change more or less in sync. Thus, our results clearly show that similar mole fractions/propensities of residues might conceal the full picture of the underlying thermodynamics.

While of utmost importance for any further modeling of peptide—solvent interactions, the obtained thermodynamic parameters alone do not assist us per se in clarifying whether or not the cosolvent actually penetrates the hydration shell and interacts directly with the peptide. However, the observation that alcohol addition also changes the spectroscopic parameters $\Delta\varepsilon_{PPII}$ and $\Delta\varepsilon_\beta$ seems to suggest that such an interaction indeed occurs. Moreover, it is reasonable to argue that a model which considers only an indirect influence of the solvent on the peptide's energy landscape (i.e., by modulation of the hydration shell) might have difficulties to explain why already a small fraction of the cosolvent can substantially affect enthalpy and entropy differences. These findings led us to conclude that glycerol and ethanol are both very effective in substituting water in the hydration shell of trialanine, thus even slightly stabilizing the PPII conformation when present at low concentrations. The notion of a direct interaction between cosolvent and peptide is further supported by the following argument. The model invoking an indirect cosolvent induced conformational stabilization is generally described in the literature by so-called "preferential hydration theories". Given that PPII conformations are known to be stabilized by water solvation (in fact PPII is not even a minimum on the free energy surface in vacuo),[49] preferential
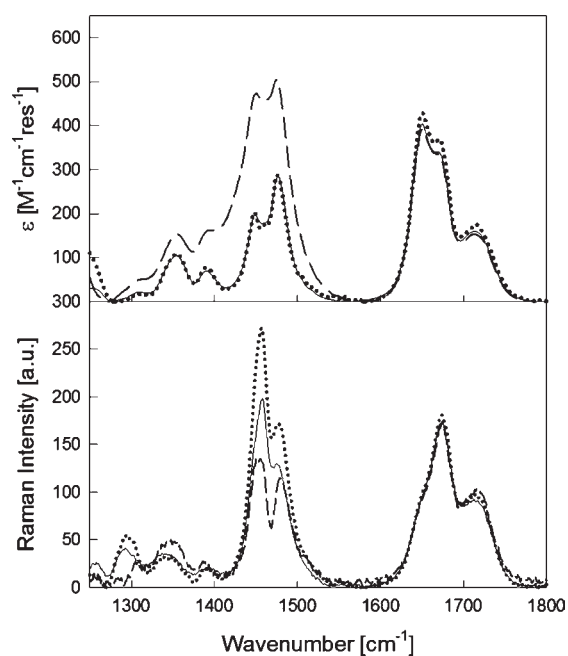
Figure 11. Infrared (upper panel) and Raman spectra (lower panel) of AAA in D_2O (solid line), 5% ethanol/D_2O (dotted line), and 5% glycerol/D_2O (dashed line).

Figure 12. DFT calculated 1418 cm^{-1} bending mode of a glycerol—alanine dipeptide complex. The right is the resting equilibrium state, and the left exhibits the maximal amplitude of the vibration.

hydration theories would argue that the addition of cosolvent may increase water content on the surface of the peptide by preferentially excluding cosolvent from the hydration shell. However, this type of indirect interaction would lead to a monotonous relationship betweeen cosolvent concentration and conformational change. This expectation is at variance with our results, namely, the initial stabilization of PPII at 5% alcohol/water mixtures followed by a shift to β-like conformations at a higher concentration cosolvent.

To investigate further the proposed direct interactions between alcohol and peptide, we measured the FT IR and Raman spectra of trialanine in water and in 5% alcohol/water (water means D_2O) mixtures. The respective spectra obtained after subtracting the respective solvent spectra are displayed in Figure 11. Apparently, the cosolvent has only a very small influence on the amide I band profiles between 1600 and 1700 cm^{-1}. This is consistent with the very small change of the PPII population inferred from our CD and NMR data. However, we observed rather dramatic intensity changes of bands in the 1300—1500 cm^{-1} region. With respect to IR, the addition of glycerol increases the intensity of nearly all bands in this region, whereas ethanol does not have a detectable effect. Both cosolvents, however, clearly affect the Raman bands particularly in the region between 1400 and 1500 cm^{-1}, which are assignable to CH_3 symmetric and antisymmetric bending modes. Bands between 1300 and 1400 cm^{-1} arise from rather complex modes with CH_3 symmetric bending and $C_\alpha H$ bending modes (in-plane and out-of-plane).[49,74,75] The substantial modification of intensity in this region of the vibrational spectra upon addition of 5% cosolvent strongly suggests that there are alcohol molecules in close enough proximity to trialanine's —CH_3 group to allow for some nonbonded, van der Waals type interaction. This would be consistent with results of recent calculations of Vagenende et al., who reported that the aliphatic part of glycerol can interact with aliphatic side chains.[60] Thus, glycerol can indeed be thought
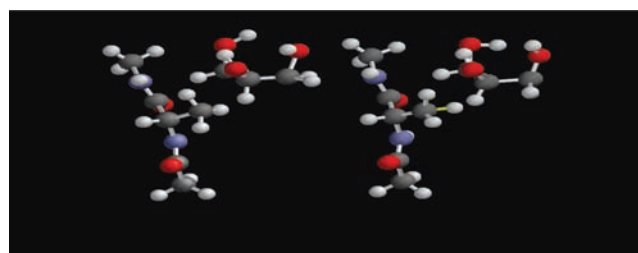
of as acting as an amphiphilc interface between hydrophobic residues and the bulk water solvent. For preferential interaction of glycerol cosolvent to occur, the glycerol molecule must be oriented such that aliphatic groups point toward peptide hydrophobic groups and the three —OH groups point toward water solvent. Our data also show that neither of the alcohols perturbs the environment of peptide's carbonyl groups.

To explain the rather strong influence of the cosolvent on IR and Raman intensities of methyl deformation modes, two options could be considered. First, one might consider drastic changes of the eigenvectors of the respective normal modes. This, however, would also cause some wavenumber shifts which have not been obtained. The second option involves vibrational mixing between solvent and peptide modes, as observed for amide I and water bending modes.[74,76] To check whether this hypothesis makes physical sense, we performed a DFT calculation for an alanine dipeptide—glycerol complex. The glycerol molecule was located close to the aliphatic CH_3 group of the central alanine residue. We used the canonical PPII coordinates ($\phi = -70°$, $\psi = 150°$) as a starting point for a structural optimization of this peptide—solvent complex on a B3LYP6-31g** level of theory. The calculation was performed with the TITAN software of Schrödinger, Inc. The optimized structure was an extended β-strand with $\phi = -161°$ and $\psi = 166°$. This result shows again that the PPII conformation is not a dominant conformaiton in the absence of water. A normal mode calculation for the optimized structure clearly revealed vibrational mixing between the symmetric CH_3 bending mode and CH as well as the OH bending mode of glycerol. This is visualized in Figure 12, which compares the equilibrium structure of an alanine dipeptide—glycerol complex with a snapshot representing the maximal amplitude of the mixed methyl—glycerol CH deformation mode.

Finally, after having provided various lines of evidence for a direct interaction between cosolvent and peptide molecules, we are now in the position to propose a model which could qualitatively describe the thermodynamic parameters derived from our data (Table 2). The nonmonotonous behavior observed for ΔH, ΔS, and the temperature coefficients of the chemical shifts with respect to their changes with increasing mole fractions of the employed cosolvents suggests different modes of peptide—alcohol interactions at low and intermediate concentrations of the latter. Since we are primarily interested in elucidating conformational propensities of nonterminal residues, we confine ourselves on considering only the data for the central residue. It seems to be reasonable to attribute these different steps to subsequent "binding" of alcohol molecules to the peptide. The term binding is justified as long as we can assume some nonbonding interactions to be operative. The first binding

of an alcohol is slightly stronger in PPII-like conformations. This provides the observed increase of the enthalpic stabilization of these conformations. The interaction potential for peptide—cosolvent pairs is describable by an anharmonic potential.[77] The corresponding vibrational energy levels are more widely spaced for the stronger bond. Thus, stronger binding to peptides in PPII conformations further increases the entropy difference between PPII and β-strand, as obtained. Higher alcohol concentrations facilitate the binding of a second and even third molecule, which for as of yet unknown reasons is stronger in the β-strand conformation. This reduces the enthalpy difference between PPII and concomitantly decreases the entropy difference between PPII and β-strand by adding more entropy to the former than to the latter. This binding model explains the behavior of ΔH and ΔS as a function of the cosolvent fraction and the above established enthalpy—entropy correlation. This model, which of course has to be confirmed by further experiments, would also involve cooperativity between the two binding steps. It would be negative for PPII and positive for β-strand.

Thus far we have not addressed one of the central issues mentioned in the Introduction, namely, the physical mechanism by which the aqueous solvent stabilizes the PPII-like conformation. We think that our results do not allow us to select any of the competing models. Liu et al. reported a linear correlation between solvent polarity and the peak intensity of the negative maximum of the CD spectra.[54] In view of the fact that these variations can reflect changes of the equilibrium between PPII and β-strand as well as changes of $\Delta\varepsilon_{PPII}$ and $\Delta\varepsilon_{\beta}$, a clear interpretation of their data is impossible without any knowledge of the underlying thermodynamics. The rather small cosolvent induced changes of the amide I' band profiles indicate that the hydration shell around the peptide groups is not substantially perturbed. This is not surprising since the above-mentioned binding of alcohol molecules to alanine side chains does not put the former into close proximity of the peptide CO and NH groups.

■ SUMMARY

In this study, we have measured and self-consistently analyzed the temperature dependence of the UV-CD spectrum and of the two $^3J(H^N,H^\alpha)$ coupling constants of trialanine in water and in binary mixtures of water with ethanol and glycerol. The thermodynamic parameters obtained from our analysis provide a rather interesting and novel picture of solvent—peptide interactions. We found that even the addition of a small fraction of alcohol (5%) causes rather substantial changes of the enthalpic and entropic differences between PPII and β-strand like conformations of the peptide but only a very small change (increase) of the PPII fraction. The addition of 30% alcohol reverses all thermodynamic parameters in a direction opposite to what we obtained for 5% alcohol/water mixtures. This causes a somewhat more pronounced but still not large destabilization of PPII. The influence of the two alcohols on enthalpic and entropic differences between PPII and the β-strand is rather different, but compensation effects between entropy and enthalpy minimize the influence on the Gibbs energy. The same observation was made by comparing the influence of the same cosolvent on the central and C-terminal residue. With respect to enthalpy and entropy, both residues behave rather differently, but the changes in Gibbs energy seem to be correlated. We found that the addition of alcohol changes the spectral parameters of the

considered conformations (i.e., PPII and β). This was interpreted as indicative of direct interactions between the cosolvent and the peptide, an observation at variance with the more preferred hydration model frequently invoked for the influence of glycerol on peptides and proteins. IR and Raman spectra of trialanine in water and in the investigated binary mixtures indeed revealed a close proximity between cosolvent molecules and the aliphatic alanine side chains of the peptide for a 5% water/alcohol mixture. We proposed a cooperative binding model for cosolvent—peptide pairs to account for the obtained thermodynamic parameters and the correlation between enthalpic and entropic differences between PPII and β strand conformations.

■ ASSOCIATED CONTENT

ⓢ **Supporting Information.** Fitting procedure for $^3J(H^N,H^\alpha)$ coupling data, H NMR chemical shift assignments, and complete references for references 3 and 61. This material is available free of charge via the Internet at at http://pubs.acs.org.

■ AUTHOR INFORMATION

Corresponding Author
rschweitzer-stenner@drexel.edu

■ ACKNOWLEDGMENT

■ REFERENCES

(1) Li, X.; Romero, P.; Rani, M.; Dunker, A. K.; Obradovic, Z. *Genome Inf.* **1999**, *10*, 30.

(2) Romero, P.; Obradovic, Z.; Li, X.; Garner, E. C.; Brown, C. J.; Dunker, A. K. *Proteins* **2001**, *42*, 38.

(3) Dunker, A.; et al. *J. Mol. Graphics Modell.* **2001**, *19*, 26.

(4) Uversky, V. N. Natively Unfolded Proteins. In *Unfolded Proteins. From Denatured to Intrinsically Disordered*; Creamer, T. P., Ed.; Nova: Nauppauge, NY, 2008.

(5) Uversky, V. N. *Eur. J. Biochem.* **2002**, *269*, 2.

(6) Tompa, P. *Trends Biochem. Sci.* **2002**, *27*, 527.

(7) Hou, L.; Shao, H.; Zhang, Y.; Li, H.; Menon, N. K.; Neuhaus, E. B.; Brewer, J. M.; Byeon, I.-J. L.; Ray, D. G.; Vitek, M. P.; Iwashita, T.; Makula, R. A.; Przybyla, A. B.; Zagorski, M. Z. *J. Am. Chem. Soc.* **2004**, *126*, 1992.

(8) Glenner, G. C.; Wong, C. W. *Biochem. Biophys. Res. Commun.* **1984**, *120*, 885.

(9) Bernado., P.; Bertoncini, C. W.; Griesinger, C.; Zweckstetter, M.; Blackledge, M. *J. Am. Chem. Soc.* **2005**, *127*, 17968.

(10) Shi, Z.; Woody, R. W.; Kallenbach, N. R. *Adv. Protein Chem.* **2002**, *62*, 163.

(11) Bai, Y.; Chung, J.; Dyson, H. J.; Wright, P. E. *Protein Sci.* **2001**, *10*, 1056.

(12) Chandrasekar, K.; Profy, A. T.; Dyson, H. J. *Biochemistry* **1991**, *30*, 9187.

(13) Dyson, H. J.; Wright, P. E. *Curr. Opin. Struct. Biol.* **1993**, *3*, 60.

(14) Dyson, H. J.; Wright, P. E. *Adv. Protein Chem.* **2002**, *62*, 311.

(15) Dyson, H. J.; Rance, M.; Houghten, R. A.; Lerner, R. A.; Wright, P. E. *J. Mol. Biol.* **1988**, *201*, 161.

(16) Wright, P. E.; Dyson, H. J.; Lerner, R. A. *Biochemistry* **1988**, *27*, 7167.

(17) Alexandrescu, A. T.; Abeygunawardana, C.; Shortle, D. *Biochemistry* **1994**, *33*, 1063.

(18) Bernado, P.; Mylonas, E.; Petoukhov, M. V.; Blackledge, M.; Svergun, D. I. *J. Am. Chem. Soc.* **2007**, *129*, 5656.

(19) Bernado, P.; Blanchard, L.; Timminis, P.; Marion, D.; Rugrok, R. W. H.; Blackledge, M. *Proc. Natl. Acad. Sci. U.S.A.* **2005**, *102*, 17002.

(20) Woutersen, S.; Hamm, P. *J. Phys. Chem. B* **2000**, *104*, 11316.

(21) Shi, Z.; Olson, C. A.; Rose, G. D.; Baldwin, R. L.; Kallenbach, N. R. *Proc. Natl. Acad. Sci. U.S.A.* **2002**, *99*, 9190.

(22) Schweitzer-Stenner, R.; Measey, T.; Hagarman, A.; Eker, F.; Griebenow, K. *Biochemistry* **2006**, *45*, 2810.

(23) Schweitzer-Stenner, R.; Measey, T. *Proc. Natl. Acad. Sci. U.S.A.* **2007**, *104*, 6649.

(24) Brant, D. A.; Flory, P. J. J. *J. Am. Chem. Soc.* **1965**, *87*, 2791.

(25) Flory, P. J. *Statistical Mechanics of Chain Molecules*; Wiley & Sons: New York, 1969.

(26) Ramachandran, G. N.; Ramachandran, C.; Sasisekharan, V. *J. Mol. Biol.* **1963**, *7*, 95.

(27) Marqusee, S.; Robbins, V. H.; Baldwin, R. L. *Proc. Natl. Acad. Sci. U.S.A.* **1989**, *86*, 5286.

(28) Chakrabartty, A.; Kortemme, T.; Baldwin, R. L. *Protein Sci.* **1994**, *3*, 843.

(29) Shi, Z. S.; Chen, K.; Liu, Z. G.; Sosnick, T. R.; Kallenbach, N. R. *Proteins: Struct., Funct., Bioinf.* **2006**, *63*, 312.

(30) Chen, K.; Liu, Z.; Zhou, C.; Bracken, W. C.; Kallenbach, N. R. *Angew. Chem., Int. Ed.* **2007**, *46*, 9036.

(31) Chen, K.; Liu, Z.; Kallenbach, N. R. *Proc. Natl. Acad. Sci. U.S.A.* **2004**, *101*, 15352.

(32) Woutersen, S.; Pfister, R.; Hamm, P.; Mu, Y.; Kosov, D. S.; Stock, G. *J. Chem. Phys.* **2002**, *117*, 6833.

(33) Schweitzer-Stenner, R. *J. Phys. Chem. B* **2009**, *113*, 2922.

(34) Hagarman, A.; Measey, T. J.; Mathieu, D.; Schwalbe, H.; Schweitzer-Stenner, R. *J. Am. Chem. Soc.* **2010**, *132*, 542.

(35) Ding, L.; Chen, K.; Santini, P. A.; Shi, Z.; Kallenbach, N. R. *J. Am. Chem. Soc.* **2003**, *125*, 8092.

(36) Makowska, J.; Rodziewicz-Motowidlo, S.; Baginska, K.; Vila, J. A.; Liwo, A.; Chmurzynski, L.; Scheraga, H. A. *Proc. Natl. Acad. Sci. U.S.A.* **2006**, *103*, 1744.

(37) Makowska, J.; Rodziewicz, S.; Baginska, K.; Makowski, M.; Vila, J. A.; Liwo, A.; Chmurzyński, L.; Scheraga, H. A. *Biophys. J.* **2007**, *92*, 2904.

(38) Schweitzer-Stenner, R.; Measey, T.; Kakalis, L.; Jordan, F.; Pizzanelli, S.; Forte, C.; Griebenow, K. *Biochemistry* **2007**, *46*, 1587.

(39) Graf, J.; Nguyen, P. H.; Stock, G.; Schwalbe, H. *J. Am. Chem. Soc.* **2007**, *129*, 1179.

(40) Verbaro, D.; Ghosh, I.; Nau, W. M.; Schweitzer-Stenner, R. *J. Phys. Chem. B* **2010**, *114*, 17201.

(41) Best, R. B.; Buchete, N. V.; Hummer, G. *Biophys. J.* **2008**, *95*, L07.

(42) Best, R. B.; Hummer, G. *J. Phys. Chem. B* **2009**, *113*, 9004.

(43) Zagrovic, B.; Lipfert, J.; Sorin, E. J.; Millett, I. S.; van Gunsteren, W. F.; Doniach, S.; Pande, V. S. *Proc. Natl. Acad. Sci. U.S.A.* **2005**, *102*, 11698.

(44) Duan, Y.; Wu, C.; Chowdury, S.; Lee, M. C.; Xiong, G.; Zhang, W.; Yang, R.; Cieplak, P.; Luo, R.; Lee, T.; Caldwell, J.; Wang, J.; Kollman, P. *J. Comput. Chem.* **2003**, *24*, 1999.

(45) Beck, D. A. C.; Alonso, D. O. V.; Inoyama, D.; Dagget, V. *Proc. Natl. Acad. Sci. U.S.A.* **2008**, *105*, 12259.

(46) Garcia, A. E.; Sanbonmatsu, K. Y. *Proc. Natl. Acad. Sci. U.S.A.* **2002**, *99*, 2782.

(47) Garcia, A. E. *Polymer* **2004**, *120*, 885.

(48) Nerenberg, P.; Head-Gordon, T. *J. Chem. Theory Comput.* **2011**, *7*, 1220.

(49) Han, W.-G.; Jakanen, K. J.; Elstner, M.; Suhai, S. *J. Phys. Chem. B* **1998**, *102*, 2587.

(50) Kentsis, A.; Mezei, M.; Gindin, T.; R., O. *Proteins: Struct., Funct. Genet.* **2004**, *55*, 493.

(51) Drozdov, A. N.; Grossfield, A.; Pappu, R. V. *J. Am. Chem. Soc.* **2004**, *126*, 2574.

(52) Law, P.; Dagett, V. *Prot. Eng., Des. Sel.* **2010**, *23*, 27.

(53) Eker, F.; Cao, X.; Nafie, L.; Griebenow, K.; Schweitzer-Stenner, R. *J. Phys. Chem. B* **2003**, *107*, 358.

(54) Liu, Z.; Chen, K.; Ng, A.; Sho, Z.; Woody, R. W.; Kallenbach, N. R. *J. Am. Chem. Soc.* **2004**, *126*, 15144.

(55) Gekko, K.; Timasheff, S. N. *Biochemistry* **1981**, *20*, 4667.

(56) Gekko, K.; Timasheff, S. N. *Biochemistry* **1981**, *20*, 4677.

(57) Timasheff, S. N. *Adv. Protein Chem.* **1998**, *51*, 355.

(58) Johnson, M. E.; Malardier-Jugroot, C.; Head-Gordon, T. *Phys. Chem. Chem. Phys.* **2010**, *12*, 393.

(59) Malardier-Jugroot, C.; Bwron, D. T.; Soper, A. K.; Johnson, M. E.; Head- Gordon, T. *Phys. Chem. Chem. Phys.* **2011**, *12*, 382.

(60) Vagenende, V.; Yap, M. G. S.; Trout, B. L. *Biochemistry* **2009**, *48*, 11084.

(61) Steinbach, P. J.; et al. *Biochemistry* **1991**, *30*, 3988.

(62) Mishra, R.; Seckler, R.; Bhat, R. *J. Biol. Chem.* **2005**, *280*, 15553.

(63) Sedwick, H.; Cameron, J. E.; Poon, W. C. K.; Egelhaaf, S. U. *J. Chem. Phys.* **2007**, *127*, 125102.

(64) Sahu, R. K.; Prakash, V. *Int. J. Food. Prop.* **2008**, *11*, 613.

(65) Dragomir, I.; Measey, T. J.; Hagarman, A. M.; Schweitzer-Stenner, R. *J. Phys. Chem. B* **2006**, *110*, 13235.

(66) Glasoe, P. K.; Long, F. A. *J. Phys. Chem.* **1960**, *64*, 188.

(67) Jentzen, W.; Unger, E.; Karvounis, G.; Shelnutt, J. A.; Dreybrodt, W.; Schweitzer-Stenner, R. *J. Phys. Chem.* **1996**, *100*, 14184.

(68) Rucker, A. L.; Pager, C. T.; Campbell, M. N.; Qualls, J. E.; Creamer, T. P. *Proteins: Struct., Funct. Genet.* **2003**, *53*, 68.

(69) Woody, R. W. *J. Am. Chem. Soc.* **2009**, *131*, 8234.

(70) Eker, F.; Griebenow, K.; Schweitzer-Stenner, R. *J. Am. Chem. Soc.* **2003**, *125*, 8178.

(71) Oh, K.-I.; Lee, K.-K.; Park, E. K.; Yoo, D.-G.; Hwang, G.-S.; Cho, M. *Chirality* **2010**, *22*, E186.

(72) Karplus, M. *J. Chem. Phys.* **1959**, *30*, 11.

(73) Eker, F.; Cao, X.; Nafie, L.; Schweitzer-Stenner, R. *J. Am. Chem. Soc.* **2002**, *124*, 14330.

(74) Chen, X. G.; Schweitzer-Stenner, R.; Asher, S. A.; Mirkin, N. G.; Krimm, S. *J. Phys. Chem.* **1995**, *99*, 3074.

(75) Schweitzer-Stenner, R.; Eker, F.; Huang, Q.; Griebenow, K.; Mroz, P. A.; Kozlowski, P. M. *J. Phys. Chem. B* **2002**, *106*, 4294.

(76) Sieler, G.; Schweitzer-Stenner, R. *J. Am. Chem. Soc.* **1997**, *119*, 1720.

(77) Dunitz, J. D. *Chem. Biol.* **1995**, *2*, 709.